Incommensurate magnetic order: A fingerprint for electronic correlations in hole-doped cuprates

Michael Klett [1,2,*] Jacob Beyer,[1,3,4] David Riegler,[1,5,†] Jannis Seufert [1,2] Peter Wölfle [5,6]
Stephan Rachel [2,4] and Ronny Thomale [1,2,‡]

[1]*Institute for Theoretical Physics, University of Würzburg, D-97074 Würzburg, Germany*
[2]*Würzburg-Dresden Cluster of Excellence ct.qmat, University of Würzburg, D-97074 Würzburg, Germany*
[3]*Institute for Theoretical Solid State Physics, RWTH Aachen University, D-52062 Aachen, Germany*
[4]*School of Physics, University of Melbourne, Parkville, VIC 3010, Australia*
[5]*Institute for Theory of Condensed Matter, Karlsruhe Institute of Technology, D-76128 Karlsruhe, Germany*
[6]*Institute for Quantum Materials and Technologies, Karlsruhe Institute of Technology, D-76021 Karlsruhe, Germany*

Intertwined charge and magnetic fluctuations in high-T_c copper oxide superconductors (cuprates) are hypothesized to be a consequence of their correlated electronic nature. Among other observables, this is apparent in the doping dependence of incommensurate magnetic order, known as the Yamada relation (YR). We analyze the Hubbard model to challenge the universality of YR as a function of interaction strength U through Kotliar-Ruckenstein slave-boson (SB) mean-field theory and truncated-unity functional renormalization group (TUFRG). While TUFRG tends to lock in to a doping dependence of the incommensurate magnetic ordering vector obtained for the perturbative weak-coupling limit, SB not only exhibits an enhanced sensitivity upon a variation of U from weak to strong coupling, but also shows good agreement with experimental data. It supports the placement of weakly hole-doped cuprates in the intermediate- to strong-coupling regime.

I. INTRODUCTION

Due to its condensed simplification and yet remarkable complexity in terms of quantum phases of matter to which it gives rise, the Hubbard model is considered the *Drosophila* of correlated condensed matter physics. With respect to copper oxide superconductors (cuprates), the Hubbard model suggests itself to even capture many rather subtle features of magnetic/charge order and superconductivity. Despite its elementary formulation and robust microscopic foundation, the Hubbard model has proven immensely challenging to solve, rendering its solution in two and more spatial dimensions a cornerstone in the quest for understanding and predicting the properties of cuprate-type materials. For instance, recent attempts to find the exact ground state are just one of many ongoing concerted efforts by the scientific community to determine the properties of the Hubbard model [1].

One of the many intriguing phenomena observed in the Hubbard model is the emergence of incommensurate magnetic spiral order, in particular for hole doping away from pristine half filling. Such a spiral is characterized by a periodic modulation of the magnetic moments, where the modulation does not have an integer number of wavelengths within the underlying lattice. While such phenomena are readily interpreted from a weak-coupling itinerant limit where the nesting, and hence the preferred magnetic ordering, continuously detunes a function of hole-doped Fermiology, the microscopic attribution of doping-dependent incommensurate magnetic order

is much more difficult in the intermediate- to strong-coupling regime. Approaching such a parametric domain of the Hubbard model from a holistic perspective calls for methods, which are (i) not limited by real-space cluster size in their resolution of incommensurability, (ii) capable of including the dynamical interplay of charge and spin fluctuations, and (iii) feature a comprehensive tunability of U. The truncated-unity functional renormalization group (TUFRG) [2–4] suggests itself as such a candidate method. Rooted in an RG scheme of electronic diagrammatic resummation, it is consistently formulated in momentum space amenable to incommensurability phenomena and couples charge and spin fluctuations at variable interaction vertex strength U. Furthermore, the Kotliar-Ruckenstein slave-boson (SB) method [5], when generalized to its spin-rotation invariant form [6], provides a highly suitable mean-field method to track incommensurate magnetic order at arbitrary doping and interaction strength U. In particular, as shown recently in a methodological revival and makeup of the method, SB can provide a detailed fluctuation profile around any kind of reference mean field [7], resolve the topology of strong correlated electron systems [8], and reach a remarkably accurate modeling of experimental evidence on incommensurate charge order in electron-doped cuprates [9].

In this paper we do two things: First, we employ TUFRG and SB to analyze the hole-doping dependence of magnetic order in the Hubbard model. As TUFRG approaches the intermediately coupled electronic regime from the perturbative weak-coupling limit, while SB additionally features certain controlled asymptotic limits in the complementary strongly coupled limit, we assume our combined assessment from both methods to accurately capture a broad range of interaction

*Contact author: michael.klett@uni-wuerzburg.de
†Contact author: david.riegler@kit.edu
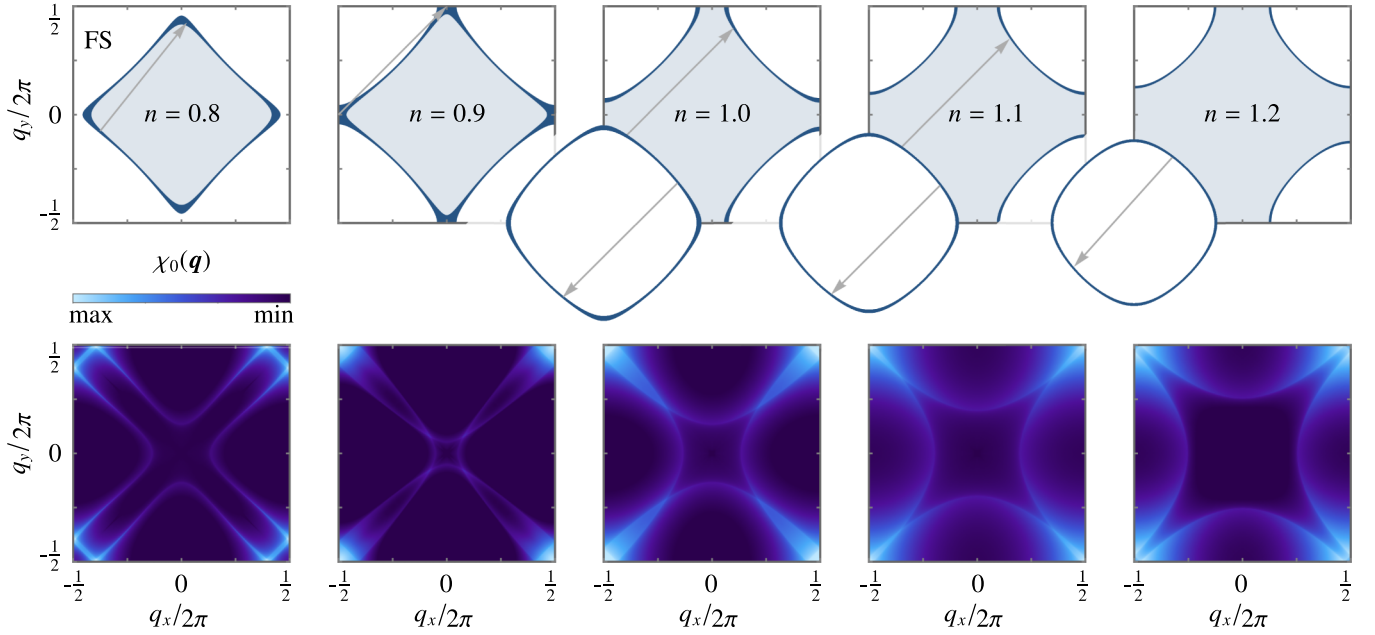‡Contact author: rthomale@physik.uni-wuerzburg.de

FIG. 1. Upper row: FS of the single-band Hubbard model Eq. (1) in the zero interaction limit at different fillings. The width of the FS indicates the density of states, and the arrow indicates the maximally nested vector of the bare susceptibilities. Lower row: Corresponding bare susceptibilities for the above FS. We can see that for sufficient doping the transfer momentum with maximal support becomes incommensurate, e.g., at $n = 0.8$ the nesting wave vector $\boldsymbol{q}/2\pi$ is shifted away from $(\frac{1}{2}, \frac{1}{2})$.

strengths. Moreover, both methods allow extracting similar observables, and hence enable a comparison on equal footing. Second, we challenge our analysis of incommensurate magnetic order with experimental evidence. In particular, this concerns the Yamada relation in hole-doped La-based cuprate materials [10], which correlates incommensurate magnetic spiral vectors with the doping level [11,12]. We find that the intermediate- to strong-coupling regime, as resolved through SB, provides the best accordance with experimental data by a significant margin.

II. MODEL

We analyze the one-band t-t'-U Hubbard model on the two-dimensional square lattice defined by

$$
H = -\sum_{\sigma=\uparrow,\downarrow} \left(t \sum_{\langle i,j\rangle_1} c_{i,\sigma}^\dagger c_{j,\sigma} + t' \sum_{\langle i,j\rangle_2} c_{i,\sigma}^\dagger c_{j,\sigma} + \text{H.c.} \right)
$$
$$
- \sum_{\sigma=\uparrow,\downarrow} \mu_0 \sum_i c_{i,\sigma}^\dagger c_{i,\sigma} + U \sum_i c_{i,\uparrow}^\dagger c_{i,\uparrow} c_{i,\downarrow}^\dagger c_{i,\downarrow}, \quad (1)
$$

where the operator $c_{i,\sigma}^\dagger$ creates an electron with spin $\sigma \in \{\uparrow, \downarrow\}$ at site i. Moreover, $\langle i, j\rangle_n$ denotes an nth nearest-neighbor pair, and μ_0 is the chemical potential. To introduce particle-hole asymmetry as experimentally observed we employ $t'/t = -0.15$ throughout the paper, which is a generic parameter in cuprate systems [13–16] and measure energy in units of t.

III. BARE SUSCEPTIBILITY

To give an initial intuition of the model and its propensity towards incommensurate order, we investigate the bare

susceptibility χ_0 which, in the absence of orbital dependencies, is equivalent to the random-phase approximation (RPA) spin susceptibility χ_s [17–19],

$$
\chi_0(\boldsymbol{q}) = \sum_k \frac{n_F(\epsilon_k) - n_F(\epsilon_{k+q})}{\epsilon_{k+q} - \epsilon_k + i0^+}, \quad \chi_s(\boldsymbol{q}) = \frac{\chi_0(\boldsymbol{q})}{1 - U\chi_0(\boldsymbol{q})}, \quad (2)
$$

with n_F representing the Fermi-Dirac distribution and ϵ_k the energy eigenvalues of Eq. (1) with $U \to 0$. The results reveal nesting properties of the undressed electrons, which stem from the Fermiology of the underlying band structure. The leading nesting vectors for a range of fillings are shown in the upper row of Fig. 1 as arrows, while the lower row depicts the corresponding susceptibilities $\chi_0(\boldsymbol{q})$. Already here, we observe the broken electron-hole symmetry: While the maxima of the susceptibility remain close to $\boldsymbol{q}/2\pi = (\frac{1}{2}, \frac{1}{2})$ for electron doping, they shift significantly on the hole-doped side. Unsurprisingly, for large dopings the warping of the Fermi surface (FS) induces incomensurabilities in the correlations, which we will compare to the TUFRG and slave-boson mean-field (SBMF) results.

IV. TRUNCATED-UNITY FRG

To investigate weak- to intermediate-coupling strengths, we employ the TUFRG. This method emphasizes the diagrammatic transfer momenta of the three channels, particle-hole, crossed particle-hole, and particle-particle, and thus captures occurring instabilities of all three. The secondary—slowly varying—momentum dependencies are projected onto basis functions $\varphi = e^{i\boldsymbol{kr}}$, with $\boldsymbol{r}$ lattice sites, to reduce computational cost. The resulting TUFRG flow equations are solved by introducing an artificial regulator, interpolating between

the high-scale no-fluctuation regime and the full-fluctuation regime at low scale. Reformulating the problem as derivatives with respect to this artificial scale Λ, we obtain an infinite hierarchy of coupled ordinary differential equations. Focusing on the two-particle terms, we can integrate the equations to obtain the effective two-particle interaction at the phase transition [4,20,21]. Neglecting further terms implies that the FS does not experience any additional warping or renormalization.

The initial condition is given by the bare action of the system at high temperature, while termination is indicated by a divergence of vertex elements and thereby defines the critical scale of $\Lambda_c \approx T_c$. The nature of the phase transition implied by the divergence, we ascertain by means of a simple eigendecomposition in the form factor space φ of the effective two-particle interaction $V_{\varphi\varphi'}^{\Lambda_c}(\boldsymbol{Q})$. The subspace of the leading eigenvalues determines the ordering vector $\boldsymbol{Q}$. If we do not encounter a divergence above a threshold scale, we determine the system to be a Fermi liquid (FL).

V. SLAVE-BOSON MEAN-FIELD APPROXIMATION

To complement the weak to intermediate coupling captured by the TUFRG, we apply the spin-rotation invariant Kotliar-Ruckenstein slave-boson representation [5,22]. This approach nonperturbatively addresses local and short-ranged density-density interactions by transforming fermionic operators c into new representations involving bosonic auxiliary fields ψ and pseudofermions f:

$$c_\alpha = Z_{\alpha\beta}[\psi]f_\beta \mathcal{P}. \tag{3}$$

Here, α and β are sets of quantum numbers uniquely labeling local states. The transformation between physical electrons and pseudofermions is governed by a renormalization matrix Z, with bosonic operators as entries [22] chosen such that the results of the Gutzwiller variational method [23] are recovered on the mean-field level. Additionally, we have to impose constraints to restore the original Hilbert space by means of projectors $\mathcal{P}$. This results in quadratic auxiliary field terms for local quartic interactions and a natural kinetic energy

scale renormalization. Pseudofermions represent quasiparticles, yielding a renormalized Fermi liquid at the mean-field level, while the condensed bosonic fields can be interpreted as probability amplitudes in the local configuration space.

To determine the ground state, we employ a static mean-field (MF) ansatz. Charge degrees of freedom are approximated as spatially uniform $\langle n_i \rangle = n$, while spin degrees are constrained to a spiral $\langle \boldsymbol{S}_i \rangle = S[\psi][\cos(\boldsymbol{Q}\boldsymbol{r}_i), \sin(\boldsymbol{Q}\boldsymbol{r}_i), 0]$ with ordering vector $\boldsymbol{Q}$, where $S \neq 0$ indicates magnetic order. Utilizing block diagonality, the MF Hamiltonian is represented by a 2×2 matrix for arbitrary $\boldsymbol{Q}$, facilitating the comparatively easy exploration of incommensurabilities [7,9,24,25]. The MF ground state is determined by the saddle point of the free energy, with the constraints enforced as thermodynamic averages.

VI. COMPARISON OF PHASE DIAGRAMS

Figure 2 illustrates the U-filling phase diagrams obtained by the TUFRG [Fig. 2(a)] and SBMF [Fig. 2(b)] methods at the critical temperature T_c of the magnetic or superconducting transition. Notably, a qualitative similarity exists between the two methods, particularly where superconductivity is suppressed by interactions, validating TUFRG's continued applicability. SBMF, being agnostic to superconducting phases, exclusively identifies magnetic phase transitions. We mention in passing that although thermal fluctuations are known to destroy long-range order in strictly two-dimensional systems (Mermin-Wagner theorem), the growth of the correlation length may trigger a phase transition in the (experimentally studied) three-dimensional systems, even for very small interlayer coupling. We identify the transition found in SBMF with such a transition.

Consistent with prior large-T SB studies of the Hubbard model [7], we observe incommensurate spiral magnetism for hole doping $\boldsymbol{Q}/2\pi = (\frac{1}{2}, \frac{1}{2} \pm \delta_s)$ and a commensurate antiferromagnetic (AFM) domain for electron doping around half filling, which matches the TUFRG results. The equivalence in the characteristics of phase diagrams validates our calculations for the weak- to intermediate-coupled regime, i.e.,
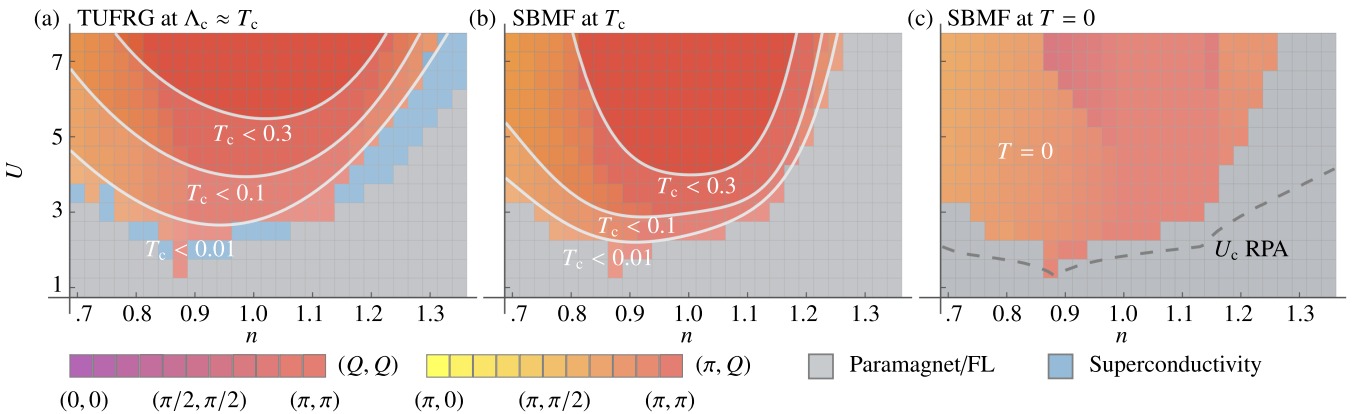

FIG. 2. (a) Phase diagrams from TUFRG at critical temperature T_c, (b) SBMF at critical temperature T_c, and (c) SBMF at zero temperature $T = 0$. The color gives the phase prediction offered by the respective methods; note that only TUFRG is capable of observing superconducting pairing instabilities. The shade of red denotes the degree of incommensurability, with purple measured along the Γ-M line and yellow measured along the X-M line. Highlighted by white contour lines in the filling interaction parameter space are fits for isothermal lines of the transition temperature T_c.
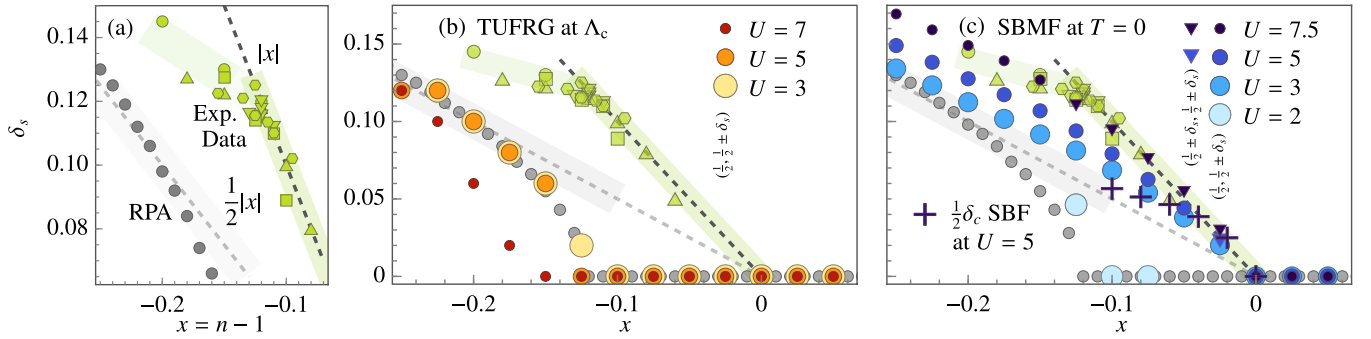
FIG. 3. (a) We compare the RPA susceptibility (gray) to experiments (green), as well as the (b) TUFRG (red) and (c) SB (blue) calculations, respectively. The experiments exhibit the Yamada relation ($\delta_s = |1 - n|$) in the hole-doped regime, reproduced by SBMF for increasing interaction, including a decreasing slope around $\delta_s \approx 0.1$. In contrast, TUFRG recovers the weak-coupling line predicted by the RPA susceptibility, but fails at high interaction strengths $U > 2$. The experimental resonant x-ray scattering (RXS) [11] (charge channel, using $2\delta_s = \delta_c$) and neutron-scattering [10] (spin channel) measurements data are taken from Ref. [30] $La_{1.8-x}Eu_{0.2}Sr_xCuO_4$ ($\square$), Ref. [10] $La_{2-x}Sr_xCuO_4$ ($\triangle$), Refs. [31–33] $La_{2-x}Sr_xCuO_4$ ($\triangledown$), Ref. [34] $La_{1.6-x}Nd_{0.4}Sr_xCu_2O_4$ ($\bigcirc$), and Refs. [35,36] $La_{2-x}Ba_xCuO_4$ ($\lozenge$).

$U \lesssim W/2$. For larger interactions, deviations in isothermal lines of the critical temperature emerge. TUFRG, due to truncation, generally underestimates critical scales for strong interactions and is in its viability is constrained to $U \approx W/2$, while SBMF, lacking fluctuation corrections, predicts higher transition temperatures [26,27].

Additionally, a SBMF phase diagram [Fig. 2(c)] at zero temperature $T = 0$ reveals incommensurate spiral magnetism with wave vectors $\boldsymbol{Q}/2\pi = (\frac{1}{2}, \frac{1}{2} \pm \delta_s)$ and $\boldsymbol{Q}/2\pi = (\frac{1}{2} \pm \delta_s, \frac{1}{2} \pm \delta_s)$ as well as a more pronounced incommensurability parameter δ_s. Notably, SBMF studies at low T suggest a phase separation of commensurate and incommensurate antiferromagnetism around half filling [25,28,29]. However, recent methodological attempts have shown that long-ranged density-density interactions significantly reduce the phase-separated domain [9]. Applying *ab initio* values for the interactions [14], we detect a phase separation for $x \lesssim 0.05$ and a continuous evolution of the incommensurability parameter δ_s as a function of doping for $x \gtrsim 0.05$ in line with the Yamada behavior.

We contrast our results with the critical interaction U_c for the spin channel predicted by RPA, which qualitatively follows the results found using TUFRG and the corresponding incommensurability parameters can be inferred from Fig. 3. Since RPA only involves the particle-hole ladder-type diagrams and does not account for all scattering processes, the overall critical scale of the system is underestimated, especially for dopings far away from the Van Hove singularity at $n \approx 0.87$, where the large density of states (DOS) at the Fermi level dominates the emerging phase transition.

To connect to experimental results, we remember that the Hubbard model is often used as a simple model of cuprate systems. This relies on the electron's confinement to the copper atoms for the electron-doped regime and the Zhang-Rice singlet [37] for the hole-doped regime. Despite its inherent simplifications and approximations, Eq. (1) has proven to be a valuable theoretical model for gaining insights into the behavior of high-temperature superconductors. To contextualize the above presented results we compare them to spin incommensurabilities measured in the La-based cuprate family.

VII. EXPERIMENTAL RESULTS AND YAMADA RELATION

Incommensurability is not merely a theoretical concept; it manifests in high-T_c cuprates. Yamada *et al.* [10] established this through neutron-scattering experiments on $La_{2-x}Sr_xCuO_4$ and showed that the low-energy spin-fluctuation peak shifts from $(\frac{1}{2}, \frac{1}{2})$ to $(\frac{1}{2} \pm \delta_s, \frac{1}{2})$ and $(\frac{1}{2}, \frac{1}{2} \pm \delta_s)$ beyond a critical hole doping ($|x| \gtrsim 0.05$). Further studies additionally revealed an incommensurate spin-density wave, along $(\frac{1}{2} \pm \delta_s, \frac{1}{2} \pm \delta_s)$, which rotates upon increased doping by 45° back to the order type reported by Yamada *et al.*, resembling the findings of the SBMF phase diagram at constant temperature [38,39]. The incommensurability parameter δ_s approximately follows the relation $\delta_s = |x|$, known as the Yamada relation.

Further investigations on related materials [32,40] show the coexistence of charge density wave and incommensurate magnetic order, where the wave vectors exhibit a simple relationship $\delta_c = 2\delta_s$. The Yamada relation is therefore sometimes expressed as in terms of the charge incommensurability $\delta_c = 2|x|$. The interplay of incommensurate charge and spin order in the Hubbard model has been studied on finite-size systems using the above SB method with similar results for δ_s Ref. [41]. A recent discussion of the quality of the above SB method can be found in Ref. [42] (Sec. II C 1). We explore charge instabilities atop commensurate magnetic order by analyzing the charge susceptibility within the SB representation and the fluctuation (SBF) formalism from Refs. [9,25]. Our results show no charge instabilities within the commensurate AFM domain but indicate a charge incommensurability accompanying the spin incommensurability, roughly following the previously mentioned behavior [compare Fig. 3(c)]. In contrast to electron doping [9,25], we find δ_c directly tied to δ_s. However, as the current formalism lacks the ability to calculate fluctuations around incommensurate ground states, these results are a reliable approximation only for small dopings and intermediate values of interaction.

Note that other cuprate families, e.g., Y- and Bi-based compounds, do not follow the Yamada relation and realize other types of spin and charge incomensurablilties [11]. For

comparison, experimental measurements [10–12,30–36] of the Yamada dependence $\delta_s \approx |x|$ stemming for charge and spin measurements are included in Fig. 3.

VIII. INCOMMENSURABILITY AS A FUNCTION OF FILLING

In Fig. 3(a), we illustrate the disparity between the observed Yamada line and the bare susceptibility calculation. The reduced incommensurability in the bare calculations can be attributed to the absence of FS warping effects, i.e., self-energy contributions. Figure 3(b) showcases the alignment of TUFRG calculations with the RPA result, especially up to couplings of $U \approx W/2$, beyond which TUFRG is deemed somewhat unreliable [43]. This underscores the presumed connection between FS behavior, as represented by the bare susceptibility, and TUFRG calculations. In contrast, SBMF results not only replicate the Yamada line at high interaction values ($U \gtrsim W/2$) but also capture the low coupling behavior seen in the bare susceptibility. Noteworthy is the presentation of these calculations at a constant temperature, resembling an experimental setup more closely. At the critical temperature, SBMF does not coincide with the Yamada line. We deduce from these findings that the renormalization of the FS, the emergence of the magnetic phase beyond the paramagnetic-magnetic transition, and substantial bare couplings are all essential factors for the establishment of the Yamada regime.

IX. CONCLUSION

We analyze the one-band Hubbard model to explore the dependence of incommensurate magnetic order on doping and interaction strength U within a wide parameter space. Comparing the results of our chosen SB and TUFRG approaches, both methods reproduce the Fermiology-driven magnetic instability already visible from the bare susceptibility. At intermediate-to-large U, it is SB that most accurately reproduces a magnetic footprint akin to the Yamada relation for hole-doped cuprates. As this is a comprehensive theoretical reproduction of this experimental phenomenology, one might expect a renaissance of SB methodology to address intricate many-body phenomena in strongly correlated electron systems.

[1] T. Schäfer, N. Wentzell, F. Šimkovic, Y.-Y. He, C. Hille, M. Klett, C. J. Eckhardt, B. Arzhang, V. Harkov, F.-M. Le Régent, A. Kirsch, Y. Wang, A. J. Kim, E. Kozik, E. A. Stepanov, A. Kauch, S. Andergassen, P. Hansmann, D. Rohe, Y. M. Vilk *et al.*, Tracking the footprints of spin fluctuations: A multi-method, multimessenger study of the two-dimensional Hubbard model, Phys. Rev. X **11**, 011058 (2021).

[2] J. Beyer, J. B. Hauck, and L. Klebl, Reference results for the momentum space functional renormalization group, Eur. Phys. J. B **95**, 65 (2022).

[3] J. Lichtenstein, D. Sánchez de la Peña, D. Rohe, E. Di Napoli, C. Honerkamp, and S. Maier, High-performance functional renormalization group calculations for interacting fermions, Comput. Phys. Commun. **213**, 100 (2017).

[4] W. Metzner, M. Salmhofer, C. Honerkamp, V. Meden, and K. Schönhammer, Functional renormalization group approach to correlated fermion systems, Rev. Mod. Phys. **84**, 299 (2012).

[5] G. Kotliar and A. E. Ruckenstein, New functional integral approach to strongly correlated Fermi systems: The Gutzwiller approximation as a saddle point, Phys. Rev. Lett. **57**, 1362 (1986).

[6] T. Li, P. Wölfle, and P. J. Hirschfeld, Spin-rotation-invariant slave-boson approach to the Hubbard model, Phys. Rev. B **40**, 6817 (1989).

[7] D. Riegler, M. Klett, T. Neupert, R. Thomale, and P. Wölfle, Slave-boson analysis of the two-dimensional Hubbard model, Phys. Rev. B **101**, 235137 (2020).

[8] M. Klett, S. Ok, D. Riegler, P. Wölfle, R. Thomale, and T. Neupert, Topology and magnetism in the Kondo insulator phase diagram, Phys. Rev. B **101**, 161112(R) (2020).

[9] D. Riegler, J. Seufert, E. H. da Silva Neto, P. Wölfle, R. Thomale, and M. Klett, Interplay of spin and charge order in the electron-doped cuprates, Phys. Rev. B **108**, 195141 (2023).

[10] K. Yamada, C. H. Lee, K. Kurahashi, J. Wada, S. Wakimoto, S. Ueki, H. Kimura, Y. Endoh, S. Hosoya, G. Shirane, R. J. Birgeneau, M. Greven, M. A. Kastner, and Y. J. Kim, Doping dependence of the spatially modulated dynamical spin correlations and the superconducting-transition temperature in La$_{2-x}$Sr$_x$CuO$_4$, Phys. Rev. B **57**, 6165 (1998).

[11] R. Comin and A. Damascelli, Resonant x-ray scattering studies of charge order in cuprates, Annu. Rev. Condens. Matter Phys. **7**, 369 (2016).

[12] S. Lee, E. W. Huang, T. A. Johnson, X. Guo, A. A. Husain, M. Mitrano, K. Lu, A. V. Zakrzewski, G. A. de la Peña, Y. Peng, H. Huang, S.-J. Lee, H. Jang, J.-S. Lee, Y. I. Joe, W. B. Doriese, P. Szypryt, D. S. Swetz, S. Chi, A. A. Aczel *et al.*, Generic character of charge and spin density waves in superconducting cuprates, Proc. Natl. Acad. Sci. USA **119**, e2119429119 (2022).

[13] T. Das, R. Markiewicz, and A. Bansil, Intermediate coupling model of the cuprates, Adv. Phys. **63**, 151 (2014).

[14] M. Hirayama, Y. Yamaji, T. Misawa, and M. Imada, *Ab initio* effective Hamiltonians for cuprate superconductors, Phys. Rev. B **98**, 134501 (2018).

[15] R. S. Markiewicz, S. Sahrakorpi, M. Lindroos, H. Lin, and A. Bansil, One-band tight-binding model parametrization of the high-T_c cuprates including the effect of k_z dispersion, Phys. Rev. B **72**, 054519 (2005).

[16] C. Honerkamp and M. Salmhofer, Temperature-flow renormalization group and the competition between superconductivity and ferromagnetism, Phys. Rev. B **64**, 184516 (2001).

[17] S. Hochkeppel, F. F. Assaad, and W. Hanke, Dynamical-quantum-cluster approach to two-particle correlation functions in the Hubbard model, Phys. Rev. B **77**, 205103 (2008).

[18] M. Altmeyer, D. Guterding, P. J. Hirschfeld, T. A. Maier, R. Valenti, and D. J. Scalapino, Role of vertex corrections in the matrix formulation of the random phase approximation for the multiorbital Hubbard model, Phys. Rev. B **94**, 214515 (2016).

[19] M. Dürrnagel, J. Beyer, R. Thomale, and T. Schwemmer, Unconventional superconductivity from weak coupling, Eur. Phys. J. B **95**, 112 (2022).

[20] J. Beyer, F. Goth, and T. Müller, Better integrators for functional renormalization group calculations, Eur. Phys. J. B **95**, 116 (2022).

[21] C. Platt, W. Hanke, and R. Thomale, Functional renormalization group for multi-orbital Fermi surface instabilities, Adv. Phys. **62**, 453 (2013).

[22] R. Frésard and P. Wölfle, Unified slave boson representation of spin and charge degrees of freedom for strongly correlated Fermi systems, Int. J. Mod. Phys. B **06**, 685 (1992).

[23] M. C. Gutzwiller, Effect of correlation on the ferromagnetism of transition metals, Phys. Rev. Lett. **10**, 159 (1963).

[24] R. Frésard, M. Dzierzawa, and P. Wölfle, Slave-boson approach to spiral magnetic order in the Hubbard model, Europhys. Lett. **15**, 325 (1991).

[25] J. Seufert, D. Riegler, M. Klett, R. Thomale, and P. Wölfle, Breakdown of charge homogeneity in the two-dimensional Hubbard model: Slave-boson study of magnetic order, Phys. Rev. B **103**, 165117 (2021).

[26] R. F. Sabiryanov and S. S. Jaswal, *Ab initio* calculations of the Curie temperature of complex permanent-magnet materials, Phys. Rev. Lett. **79**, 155 (1997).

[27] B. Peng and Y.-X. Yu, A density functional theory with a mean-field eeight function: Applications to surface tension, adsorption, and phase transition of a Lennard-Jones fluid in a slit-like Pore, J. Phys. Chem. B **112**, 15407 (2008).

[28] P. Igoshev, M. Timirgazin, A. Arzhnikov, and V. Irkhin, Effect of electron correlations on the formation of spiral magnetic states in the two-dimensional t-t' Hubbard model, JETP Lett. **98**, 150 (2013).

[29] P. A. Igoshev, M. A. Timirgazin, V. F. Gilmutdinov, A. K. Arzhnikov, and V. Y. Irkhin, Spiral magnetism in the single-band Hubbard model: The Hartree–Fock and slave-boson approaches, J. Phys.: Condens. Matter **27**, 446002 (2015).

[30] J. Fink, E. Schierle, E. Weschke, J. Geck, D. Hawthorn, V. Soltwisch, H. Wadati, H.-H. Wu, H. A. Dürr, N. Wizent, B. Büchner, and G. A. Sawatzky, Charge ordering in La$_{1.8-x}$Eu$_{0.2}$Sr$_x$CuO$_4$ studied by resonant soft x-ray diffraction, Phys. Rev. B **79**, 100502(R) (2009).

[31] H.-H. Wu, M. Buchholz, C. Trabant, C. Chang, A. Komarek, F. Heigl, M. Zimmermann, M. Cwik, F. Nakamura, M. Braden, and C. Schüßler-Langeheine, Charge stripe order near the surface of 12-percent doped La$_{2-x}$Sr$_x$CuO$_4$, Nat. Commun. **3**, 1023 (2012).

[32] T. P. Croft, C. Lester, M. S. Senn, A. Bombardi, and S. M. Hayden, Charge density wave fluctuations in La$_{2-x}$Sr$_x$CuO$_4$ and their competition with superconductivity, Phys. Rev. B **89**, 224513 (2014).

[33] N. B. Christensen, J. Chang, J. Larsen, M. Fujita, M. Oda, M. Ido, N. Momono, E. M. Forgan, A. T. Holmes, J. Mesot, M. Huecker, and M. v. Zimmermann, Bulk charge stripe order competing with superconductivity in La$_{2-x}$Sr$_x$CuO$_4$ ($x = 0.12$), arXiv:1404.3192.

[34] J. M. Tranquada, J. D. Axe, N. Ichikawa, A. R. Moodenbaugh, Y. Nakamura, and S. Uchida, Coexistence of, and competition between, superconductivity and charge-stripe order in La$_{1.6-x}$Nd$_{0.4}$Sr$_x$CuO$_4$, Phys. Rev. Lett. **78**, 338 (1997).

[35] P. Abbamonte, A. Rusydi, S. Smadici, G. D. Gu, G. A. Sawatzky, and D. L. Feng, Spatially modulated 'Mottness' in La$_{2-x}$Ba$_x$CuO$_4$, Nat. Phys. **1**, 155 (2005).

[36] M. Hücker, M. v. Zimmermann, Z. J. Xu, J. S. Wen, G. D. Gu, and J. M. Tranquada, Enhanced charge stripe order of superconducting La$_{2-x}$Ba$_x$CuO$_4$ in a magnetic field, Phys. Rev. B **87**, 014501 (2013).

[37] F. C. Zhang and T. M. Rice, Effective Hamiltonian for the superconducting Cu oxides, Phys. Rev. B **37**, 3759 (1988).

[38] R. Comin, A. Frano, M. M. Yee, Y. Yoshida, H. Eisaki, E. Schierle, E. Weschke, R. Sutarto, F. He, A. Soumyanarayanan, Y. He, M. L. Tacon, I. S. Elfimov, J. E. Hoffman, G. A. Sawatzky, B. Keimer, and A. Damascelli, Charge order driven by Fermi-arc instability in Bi$_2$Sr$_{2-x}$La$_x$CuO$_{6+\delta}$, Science **343**, 390 (2014).

[39] L. Chaix, E. W. Huang, S. Gerber, X. Lu, C. Jia, Y. Huang, D. E. McNally, Y. Wang, F. H. Vernay, A. Keren, M. Shi, B. Moritz, Z.-X. Shen, T. Schmitt, T. P. Devereaux, and W.-S. Lee, Resonant inelastic x-ray scattering studies of magnons and bimagnons in the lightly doped cuprate La$_{2-x}$Sr$_x$CuO$_4$, Phys. Rev. B **97**, 155144 (2018).

[40] M. Hücker, M. v. Zimmermann, G. D. Gu, Z. J. Xu, J. S. Wen, G. Xu, H. J. Kang, A. Zheludev, and J. M. Tranquada, Stripe order in superconducting La$_{2-x}$Ba$_x$CuO$_4$ ($0.095 \leqslant x \leqslant 0.155$), Phys. Rev. B **83**, 104506 (2011).

[41] M. Raczkowski, R. Frésard, and A. Oleś, Interplay between incommensurate phases in the cuprates, Europhys. Lett. **76**, 128 (2006).

[42] L. Philoxene, V. H. Dao, and R. Frésard, Spin and charge modulations of a half-filled extended Hubbard model, Phys. Rev. B **106**, 235131 (2022).

[43] C. Hille, F. B. Kugler, C. J. Eckhardt, Y.-Y. He, A. Kauch, C. Honerkamp, A. Toschi, and S. Andergassen, Quantitative functional renormalization group description of the two-dimensional Hubbard model, Phys. Rev. Res. **2**, 033372 (2020).